Grant agreement no. 667510

GLINT

Research and Innovation Action
H2020-PHC-2015-two-stage

D5.1 Assessment of in vitro magnetic field dependence properties

Work Package:	5
Due date of deliverable:	30/06/2016
Actual submission date:	June 30, 2016
Lead beneficiary:	
Contributors:	
Reviewers:	

Project co-funded by the European Commission within the H2020 Programme (2014-2020)		
Dissemination Level		
PU	Public	YES
CO	Confidential, only for members of the consortium (including the Commission Services)	
CI	Classified, as referred to in Commission Decision 2001/844/EC	

*"This project has received funding from the European Union's Horizon 2020 research and innovation programme under the Grant Agreement No **667510**"*

Disclaimer

The content of this deliverable does not reflect the official opinion of the European Union. Responsibility for the information and views expressed herein lies entirely with the author(s).

*"This project has received funding from the European Union's Horizon 2020 research and innovation programme under the Grant Agreement No **667510**"*

Contents

*"This project has received funding from the European Union's Horizon 2020 research and innovation programme under the Grant Agreement No **667510**"*

1 Introduction

The CEST contrast attainable with the investigated molecules (glucose and 3OMG) is dependent on several conditions, including temperature, concentration, saturation power level (B_1) and magnetic field strength (B_0). The aim of this task is to assess the influence of all these factors on the CEST contrast, to elucidate their contribution and to assess the detection limits of these CEST agents.

The chemical exchange rate is dependent on the pH of the solution where the molecule is dissolved, therefore a throughout evaluation of the CEST contrast will be performed in the range of physiological pH. In particular, considering that these molecules have been proposed for oncological applications, pH values in the range of 6.0-7.4 will be investigated. These values have been chosen in order to investigate the low extracellular pH values that may be encountered in the extracellular extravascular space of tumors, when they extravasate, and the close to neutral pH values that are found intracellular, once the molecules have been taken up by tumor cells.

Due to the relative small chemical shift of hydroxyl protons, a huge dependence of the contrast is to be expected according to the magnetic field and to the saturation power levels. In fact, at lower magnetic field (3T, as available in clinics), the separation is hertz between the hydroxyl protons and the bulk water protons is reduced, in comparison to the high magnetic field of preclinical scanners (7T). As a consequence, direct saturation of the bulk water pool may reduce the efficient labeling of the hydroxyl protons, hence reducing their contrast efficiency. These effects will be investigated by acquiring images at different magnetic fields (3T and 7T) and at different B_1 power levels (range: 1 μT – 3 μT).

Detection of CEST agents usually requires the accumulation in the region of interest in the order of mM concentration. We will investigate the detection threshold, i.e. the lower concentration that is still detectable, considering a threshold value of 2% of CEST contrast. Because of the CEST contrast is affected by several parameters, a range of concentrations that have been shown to be achievable inside tumors (2.5-20 mM) will be investigated. Moreover, we will investigate the influence of pH by preparing solutions at different concentration and pH values.

All the above mentioned factors will provide a detailed description of the GlucoCEST contrast, allowing a precise characterization of the CEST properties of the investigated molecules.

*"This project has received funding from the European Union's Horizon 2020 research and innovation programme under the Grant Agreement No **667510**"*

2 Methodology and Approach for

Phantoms containing different vials of phosphate buffered solutions of D-Glucose and 3-O-methyl-D-glucose at several pH values were prepared starting from a 20 mM solution of D-Glucose (Sigma-Aldrich) or 3-O-methyl-D-glucose (Sigma-Aldrich) at neutral pH (pH7.4); then the solution was titrated at pH of 7.0, 6.8, 6.6, 6.4, 6.2 and 6.0 and each vials filled. Phantoms containing vials of phosphate buffered solutions of D-Glucose and 3-O-methyl-D-glucose at variable concentration were prepared starting from a 20mM solution at pH 7.4 and 6.8 and then diluted (10, 5 and 2.5mM). A solution of 20mM of D-Glucose and 3-O-methyl-D-glucose was chosen for a direct comparison with already published data.

Z-spectra were acquired on a BrukerBioSpec 3T and Bruker Avance 300 (7T) equipped with a micro2.5 imaging probe. The experiments were obtained at 37°C and 21°C by irradiating the sample with a single continuous wave presaturation block pulse (from 1 to 3 μT) applied for 5 sec. The saturation frequency offset was varied between 10 and -10 ppm with a frequency resolution of 0.1 ppm. MR images were acquired using a Spin Echo RARE sequence (TR/TE/NEX/Rare Factor 10.0 sec/5.4 msec/2/64); centric encoding, field of view = 3 cm x 3 cm; slice thickness = 2 mm; matrix =64 x 64.

All the CEST images were elaborated in MATLAB (The Mathworks, Inc., Natick, MA, USA) using custom scripts. Anatomical and Z-spectrum images were first segmented by the use of an intensity-threshold filter **(1)**. The Z-spectra were interpolated, on a voxel-by-voxel basis, by smoothing splines **(2)** to identify the correct position of the bulk water, thus removing artefacts arising from B_0 inhomogeneity. On this basis, the interpolated Z-spectrum was shifted so that the bulk water resonance corresponds to the zero frequency and corrected intravoxel saturation transfer (ST) effects were calculated. Then, a second filter was applied to remove CEST effect arising from noisy data, calculating the coefficient of determination R^2 for the interpolating curve to take into account the signal-to-noise ratio of single voxels (noisy Z-spectra present low R^2 values). Only voxels with high R^2 (>0.99) were considered in the ST% calculation.

*"This project has received funding from the European Union's Horizon 2020 research and innovation programme under the Grant Agreement No **667510**"*

3 Report Activities carried-out and results

To assess the in vitro magnetic field dependence properties of D-Glucose and 3-O-methyl-D-glucose, phantoms containing the solutions titrated at variable pH and at different concentration were investigated. Z-Spectra were acquired at two different MRI scanner: high field 7T scanner and a preclinical scanner working at clinical field of 3T. It was chosen a chemical shift of 0.8 ppm and 1.2 ppm to D-Glucose and 3-O-methyl-D-glucose respectively, in order to obtain a higher signal.

3.1.1 Results at 7T, T=21°C

1

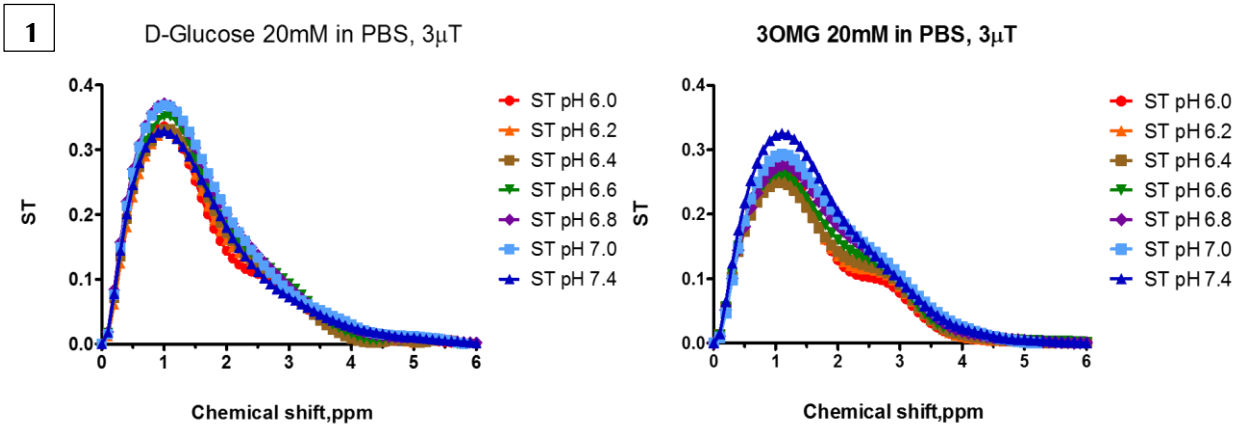

2

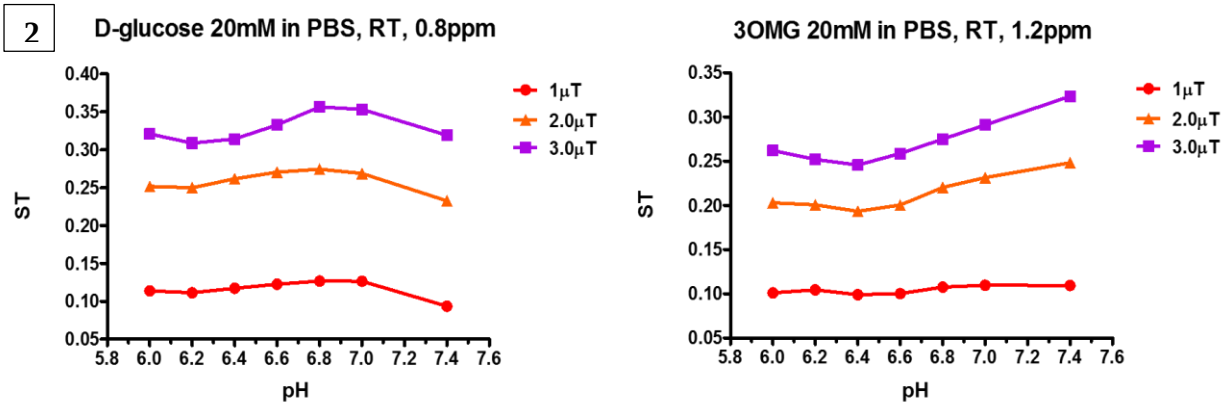

Z-Spectra of 20mM D-Glucose solutions at variable pH acquired at 7T, 3µT saturation pulse and 21°C showed a higher ST effect at pH between 6.6 and 7.0 (ST effect close to 40%). 3OMG displayed a lower CEST effect (ST higher than 30% at pH 7.4).

Figure 2 shows the CEST curves obtained at temperature 21°C and a frequency of 0.8ppm and 1.2ppm for 20mM D-Glucose and 3-O-methyl-D-glucose solutions respectively, plot with pH values from 5.8-7.4 and rf saturation fields value. The highest ST value for the D-glucose is displayed at pH 6.8 and right after it decreased as the pH became neutral. 3OMG showed an

*"This project has received funding from the European Union's Horizon 2020 research and innovation programme under the Grant Agreement No **667510**"*

increased in the ST effect at lower pH than D-glucose (6.6) and it increases, as the pH became more neutral using higher saturation pulse.

3.1.2 Results at 7T, T=21°C and variable concentration

3

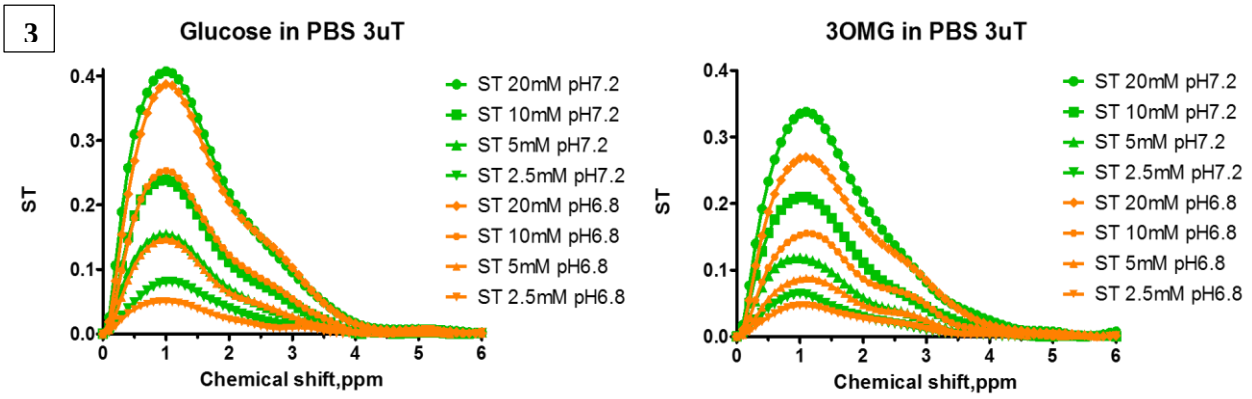

Figure 3 shows the CEST effect for phantoms containing D-Glucose and 3-O-methyl-D-glucose solutions at variable concentration (20,10,5 and 2.5mM) titrated at pH7.2 and 6.8 acquired at 7T at temperature 21°C with a 3µT saturation pulse. The ST values for solution of D-glucose at the same concentration reached the maximum value at 20mM and pH 7.2 – 6.8 and it decreased as the concentration decreased. The difference between the same concentration solutions at different pH is grater in 3OMG and the ST effect decreased as the concentration decreased.

4

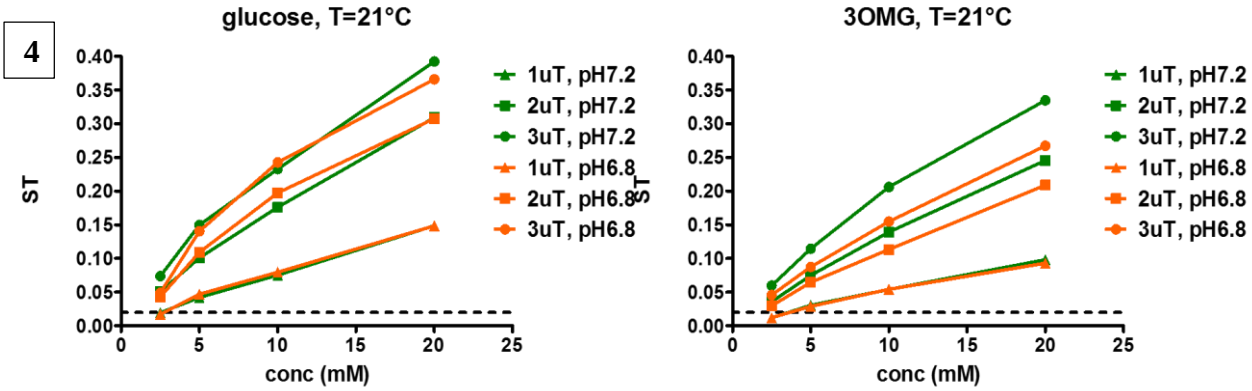

Figure 4 displays the detection threshold fixed at 2% for D-glucose and 3-O-methyl-D-glucose at 21°C. D-glucose and 3-O-methyl-D-glucose 2.5mM at pH 6.8 and 7.2 are not easily detectable using a 1µT saturation pulse; increasing the saturation pulse even lower concentration are detectable (D-glucose greater than 5% of ST signal and between 2 and 5% for 3-O-methyl-D-glucose) in a similar fashion at different pH. D-glucose solutions at higher concentration has an increased ST effect and in particular reaches values close to 25% the

*"This project has received funding from the European Union's Horizon 2020 research and innovation programme under the Grant Agreement No **667510**"*

solution 10mM D-glucose, pH 6.8 at 3µT but the maximum St effect is obtained at 3µT 20mM D-glucose pH7.2 (40%). Conversely 3-O-methyl-D-glucose has an increased ST effect that reaches higher values at pH more neutral than D-glucose. The maximum ST effect (30%) is reached at 3µT, 20mM 3OMG solution titrated at pH 7.2. Both the molecule has an increase in the CEST effect as the concentration increases, but D-glucose shows a clearer signal at lower concentration.

3.1.3 Results at 7T, T=37°C

5

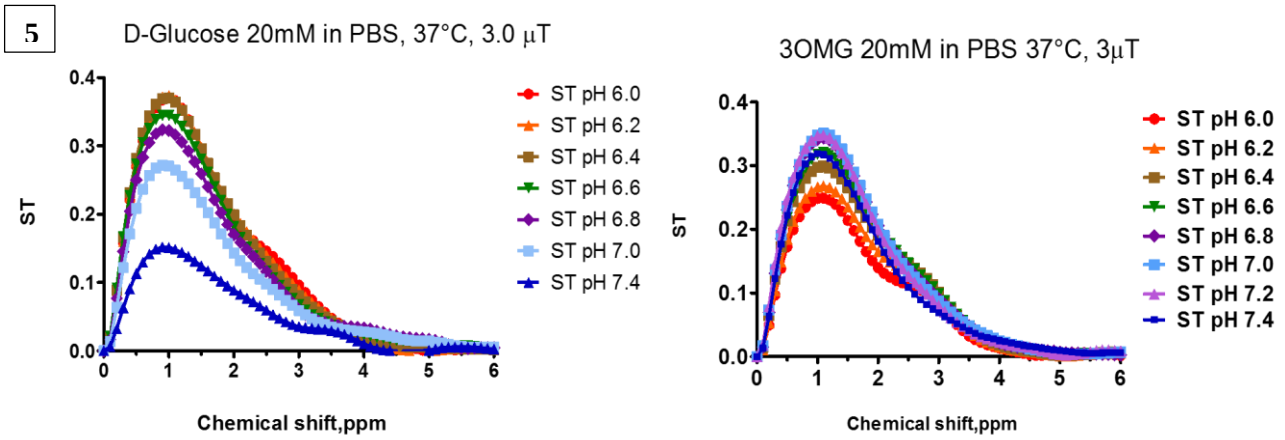

6

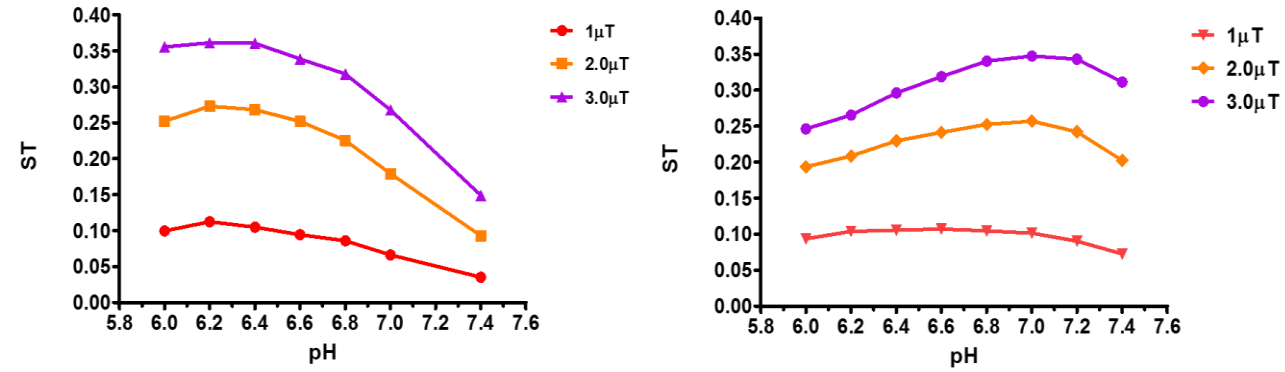

At 37°C (Figure 5) with 3µT of saturation pulse the CEST effect of D-glucose reached 36% between pH6.4 and 6.0 instead the 3OMG reached higher CEST effect at neutral pH (7.2-6.8 pH).

Figure 6 shows the CEST curves obtained at temperature 37°C and a frequency of 0.8ppm and 1.2ppm for 20mM D-Glucose and 3-O-methyl-D-glucose solutions respectively, plot with pH values from 5.8-7.4 and rf saturation fields value.

*"This project has received funding from the European Union's Horizon 2020 research and innovation programme under the Grant Agreement No **667510**"*

3.1.4 Results at 7T, T=37°C and variable concentration

7

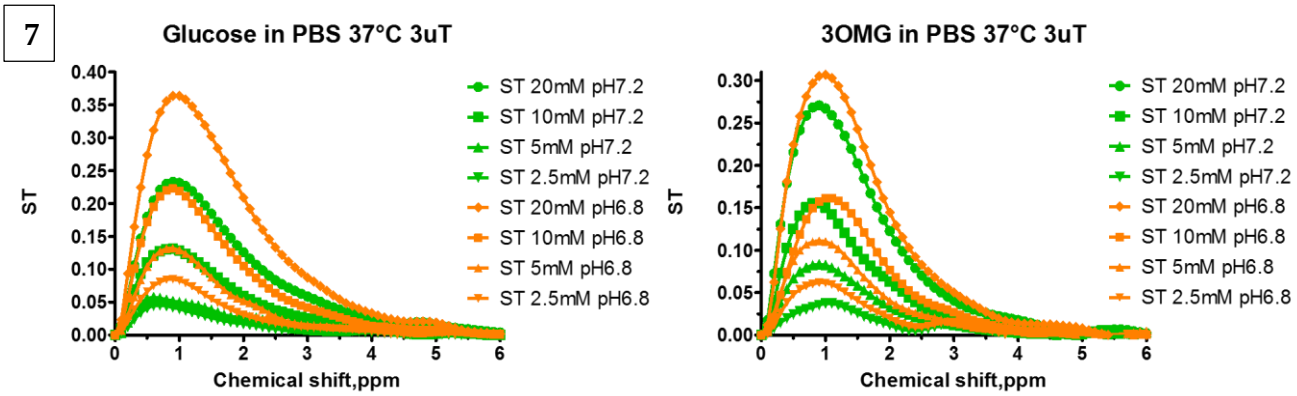

Figure 7 shows the CEST effect for phantoms containing D-Glucose and 3-O-methyl-D-glucose solutions at variable concentration (20,10,5 and 2.5mM) titrated at pH7.2 and 6.8 acquired at 7T at temperature 37°C with a 3μT saturation pulse. The maximum ST effect is observed at pH 6.8 both for D-glucose and 3OMG with 20mM concentration.

8

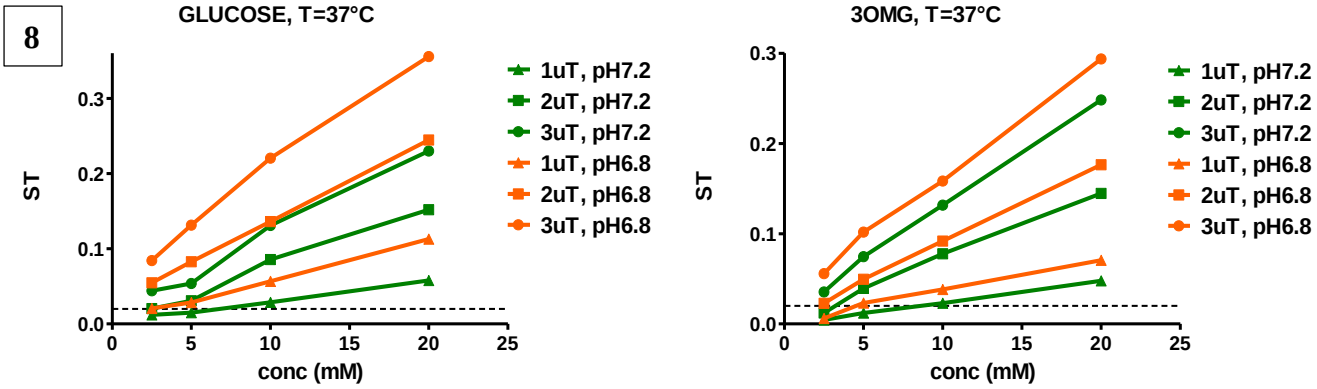

Figure 8 displays the detection threshold fixed at 2% for D-glucose and 3-O-methyl-D-glucose at 37°C. Lower concentrations of D-glucose and 3-O-methyl-D-glucose (2.5 and 5mM) have the ST effect greater than 2% only if irradiated with a 2 and 3μT saturation pulse which is between 5 to 10%. The signal is higher for solution titrated at less neutral pH than pH 7.2 and it increases as the concentration increases. Solutions with a concentration of 10-20mM of both the molecules are easily detectable using 1μT saturation pulse but the signal derived from D-glucose is higher than the 3-O-methyl-D-glucose at the same experimental condition.

*"This project has received funding from the European Union's Horizon 2020 research and innovation programme under the Grant Agreement No **667510**"*

3.2.1 Results at 3T, T=21°C

9

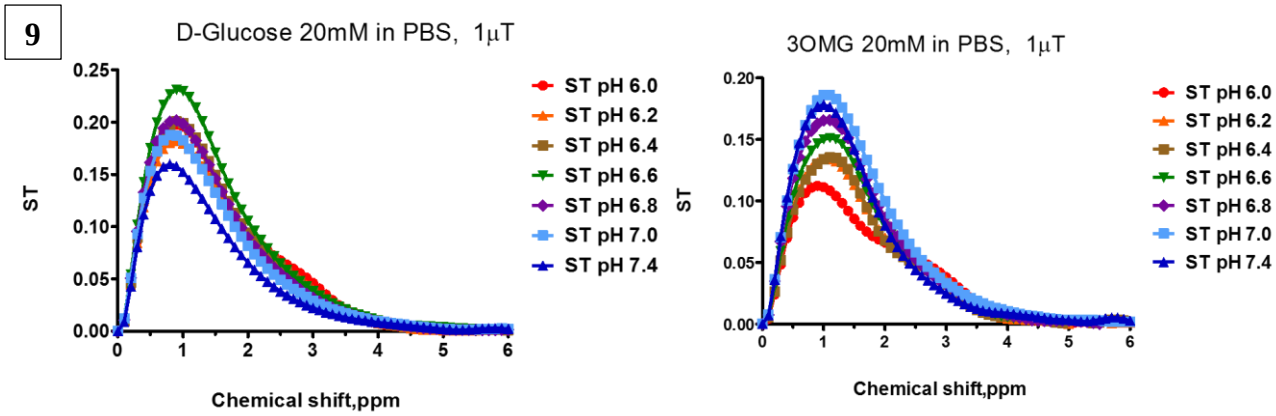

Figure 9 shows the CEST effect for phantoms containing 20mM D-Glucose and 3-O-methyl-D-glucose solutions at different pH acquired at 3 T at temperature 21°C with a 1μT saturation pulse. The highest ST effect (close to 25%) for D-Glucose was observed at 6.6 pH; 3OMG at the same acquisition condition showed an higher ST effect than the D-glucose (greater than 18%) at neutral pH (7.0) and it decreased as well as decreased the pH. The ST effect of both the solution is higher at neutral pH but pH dependence is less apparent.

3.2.2 Results at 3T, T=21°C and variable concentration

D-Glucose and 3-O-methyl-D-glucose solutions at variable concentration acquired at 3T at temperature 21°C with a 1μT saturation pulse display a different trend than at 7T. Specifically, D-glucose has a signal ST greater than 2% threshold starting from 5mM of concentration, it is higher at less acidic pH and reaches the maximum at 20mM and pH6.8. 3-O-methyl-D-glucose shows signal ST greater than the threshold at 10mM of concentration and it is higher at neutral pH.

*"This project has received funding from the European Union's Horizon 2020 research and innovation programme under the Grant Agreement No **667510**"*

4 Conclusions

A marked different dependence with pH has been observed for glucose and 3OMG. In particular, glucose provides higher CEST contrast at lower pH values, whereas 3OMG provides higher CEST contrast at pH values close to 7.0-7.4. This different behavior is quite independent from the applied B_1 saturation power level. At 7T and physiological temperature (37°C), the detection threshold is of ca. 5 mM, for a B_1 level of 1 μT.

*"This project has received funding from the European Union's Horizon 2020 research and innovation programme under the Grant Agreement No **667510**"*

5 Bibliography / References

1. Chu V, Hamarneh G. MATLAB–ITK interface for medical image filtering, segmentation, and registration. Proc SPIE Med Imaging: Image Process 2006;6144:1–8.

2. Stancanello J, Terreno E, Castelli DD, Cabella C, Uggeri F, Aime S. Development and validation of a smoothing-splines-based correction method for improving the analysis of CEST-MR images. Contrast Media Mol Imaging 2008;3:136–149.

*"This project has received funding from the European Union's Horizon 2020 research and innovation programme under the Grant Agreement No **667510**"*